Journal of Materials Chemistry C

PAPER

View Article Online
View Journal | View Issue

Cite this: J. Mater. Chem. C, 2014, 2, 4928

Investigation into the role of the hydrogen bonding network in cyclodextrin-based self-assembling mesophases†

Sandra Ward,[a] Oliver Calderon,[b] Ping Zhang,[a] Matthew Sobchuk,[a] Samantha N. Keller,[a] Vance E. Williams[b] and Chang-Chun Ling*[a]

Received 6th March 2014
Accepted 31st March 2014

DOI: 10.1039/c4tc00448e

www.rsc.org/MaterialsC

A series of novel amphiphilic β-CD derivatives capable of forming hydrogen bonding networks of different strengths have been synthesized to probe the role of the hydrogen bonding network in the formation of self-assembled mesophases. Using differential scanning calorimetry (DSC), cross-polarized optical microscopy (POM) and X-ray diffractometry, two compounds were found to exhibit smectic mesophases. These correlated well with their abilities to form a hydrogen bonding network with sufficient strength to self-assemble. It was also observed that modifying the secondary face to interfere with the hydrogen bonding network significantly affects the T_c of a CD amphiphiles while the T_m temperature was not greatly affected.

Introduction

Self-assembly of simple building blocks *via* non-covalent forces into larger ordered structures has been a hot topic of research for the last 30 years.[1] Many functional systems such as liquid crystals have been successfully designed with small molecular building blocks (mesogens) that use intermolecular forces[2–4] such as van der Waals, hydrogen bonding, π–π interaction and ionic forces. The formation of liquid crystalline (LC) phases relies heavily on the ability of the mesogenic molecules to self-assemble into highly ordered structures. Carbohydrate-based mesogens are of particular interest because of their low cost, availability of a wide range of starting materials, and accessibility of many developed chemical methods for carrying out structure modifications.[5–7] Typically, monosaccharides are transformed into mesogens by the addition of one or more aliphatic chains, generating amphiphilic molecules that self-assemble into periodically layered structures. The non-polar alkyl chains of numerous molecules self-associate to form hydrophobic regions while their polar carbohydrate head groups form hydrophilic regions. The thermotropic liquid crystalline phase that is created by this type of packing is known as the smectic (Sm) phase. Despite the presence of numerous chiral centres in a carbohydrate molecule, amphiphilic carbohydrate mesogens rarely form chiral mesophases.

Cyclodextrin (CD)-based mesogens[8] are of particular interest for LC research, as the truncated cone-shaped CD cores have a cyclic bidimensional geometry. The three common members, α-, β- and γ-CDs, form similar rigid structures with primary hydroxyl groups (OH-6's) found at the narrow end and secondary hydroxyl groups (OH-2's and OH-3's) at the wider end. The difference in reactivity between the two classes of hydroxyl groups has been exploited to regioselectively introduce functional groups.[9] In 1993, Darcy *et al.* synthesized[10] a series of 6-thioalkylated β-CD derivatives containing different chain lengths (Fig. 1).

They found that these CD amphiphiles exhibited thermotropic LC properties – especially the *n*-hexadecylthio- and *n*-octadecylthio-substituted derivatives (**1** and **2**), which displayed liquid crystallinity in a wide temperature range (215 °C to 280 °C). Upon heating, both compounds decomposed before

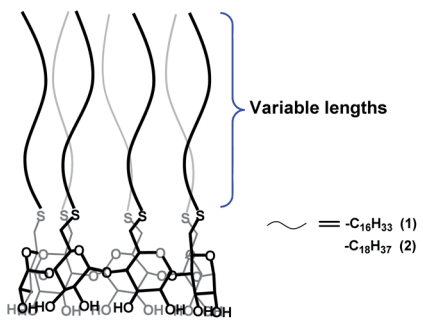

Fig. 1 Schematic structures of previously synthesized β-CD derivatives exhibiting thermotropic LC properties.

[a]Department of Chemistry and Alberta Glycomics Centre, University of Calgary, Calgary, AB T2N 1N4, Canada. E-mail: ccling@ucalgary.ca; Fax: +1 403-289-9488; Tel: +1 403-220-2768

[b]Department of Chemistry, Simon Fraser University, Burnaby, BC V5A 1S6, Canada

† Electronic supplementary information (ESI) available: Experimental details for compounds **10–25**. ^{1}H and ^{13}C NMR spectra of all synthesized compounds and DSC thermograms of compounds **3**, **4**, **7** and **8** and TGA traces of compounds **5** and **6**. See DOI: 10.1039/c4tc00448e

clearing into an isotropic liquid. Powder X-ray diffraction (XRD) revealed that the bilayers formed by **1** had a thickness of 38 Å, which is shorter than twice the molecular dimension (2 × 28 Å) of **1** in the extended conformation.

Interestingly, since the first publication, there has been only one other publication reporting a β-CD derivative with thermotropic LC properties. Zhang *et al.* introduced[11a] seven hydrophobic groups terminated with a methoxy-biphenyl moiety to the primary face of β-CD *via* the Huisgen 1,3-dipolar cycloaddition reaction, and observed that the compound entered into LC phases starting at 115 °C and cleared into an isotropic liquid at 197 °C. Using XRD, it was found that the molecule formed Sm phases. The interesting part of their design was the introduction of a common mesogenic group (4′-methoxybiphenyl group) which apparently enhanced the LC properties of the synthesized β-CD derivative. In addition, Terao *et al.*[11b] also reported that an inclusion complex of permethylated cyclodextrin with a linear polymer formed a cholesteric phase (mesophase) in concentrated chloroform.

All of the above mentioned systems exhibited LC phases that extended up to very high temperatures prior to clearing or decomposition. We hypothesized that this might be due to the strong hydrogen bonding network established between the hydroxyl groups on the secondary face of adjacent layers. The flat secondary face of CDs allows for the proper spatial arrangement and orientation for hydroxyl groups to interact in a strong and cooperative manner. Herein, several novel 6-thioalkylated β-CD derivatives (**3–8**, Fig. 2) were designed and synthesized for a systematic structure–property relationship study of hydrogen bonding ability on LC phase formation.

Results and discussion

The per-2,3-*O*-benzyl- and methyl-substituted β-CD derivatives **3** and **4** were designed because both molecules lack the ability to form intermolecular hydrogen bonds due to the absence of hydrogen bond donors. Direct information on whether the presence of hydrogen bonding is necessary for self-assembly into LC phases would be provided from these compounds. Compounds **5–8** were designed to have seven of the fourteen secondary hydroxyl groups (the OH-2's) blocked with alkyl groups of different sizes (methyl, ethyl, allyl and benzyl). All these amphiphilic polyols should be capable of forming hydrogen bonds; however, in a layered LC phase, the average distance of adjacent layers is defined by the bulkiness of alkyl groups introduced at the O-2's; consequently, the average distance between the OH-3's of adjacent layers varies, which should result in hydrogen bonds of different strengths.

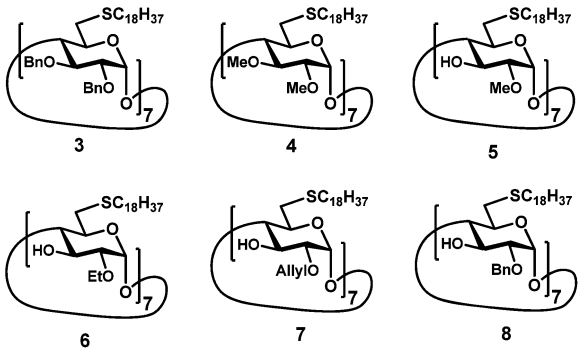

Fig. 2 Thioalkylated CD targets **3–8** designed to study the structure–property relationship between hydrogen bonding and LC phase formation.

Synthesis

The per-2,3-di-*O*-benzylated CD **3** was synthesized from the previously known per-2,3,6-tri-*O*-benzylated β-CD (**9**).[12] Among the three types of benzyl groups present in **9**, only those attached to O-6's are primary and therefore experience less steric hindrance and can be selectively modified. A procedure was reported by Utille and co-workers in 1991[13] which involved the use of acetolysis conditions on per-2,3,6-*O*-benzylated α-CD. The O-6-benzyl protecting groups were regioselectively cleaved and converted to acetate groups. Interestingly, this selective and high yielding reaction has been largely underexploited except for a recent report.[14] We were interested in applying this reaction to our synthesis (Scheme 1).

Using trimethylsilyl trifluoromethanesulfonate (TMSOTf) and acetic anhydride as reagents, it was found that the acetolysis worked very well. The reaction was carried out in anhydrous dichloromethane at −40 °C for one hour; sodium bicarbonate was added to quench the reaction, and the desired per-6-*O*-acetate **10** was obtained in 78% by column chromatography on silica gel. The 6-*O*-acetyl groups of **10** were then removed by employing Zemplén transesterification conditions to provide the polyol **11** in a quantitative yield. The 6-OH groups were then activated with methanesulfonyl chloride in a mixture of pyridine–dichloromethane to afford the desired per-6-*O*-mesylate (**12**) in 90% yield. The mesyl groups were finally replaced after a nucleophilic attack by the potassium 1-octadecanethiolate which was generated *in situ* by the treatment of 1-octadecanethiol with potassium *tert*-butoxide in DMF; the desired target **3** was obtained in 76% yield.

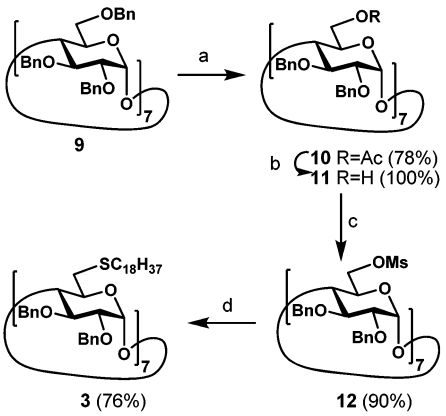

a. Ac_2O, TMSOTf/CH_2Cl_2, -40 °C; b. NaOMe, THF-MeOH;
c. MsCl/DMAP/Pyr-CH_2Cl_2; d. $HSC_{18}H_{37}$ /K^+-OBu-*t* /THF.

Scheme 1 Synthesis of per-2,3-di-*O*-benzylated β-CD **3** from **9**.

The per-2,3-di-*O*-methylated analogue (**4**) was synthesized in an analogous manner (Scheme 2) from the previously known compound **13** (ref. 15) *via* per-2,3-di-*O*-methyl-6-*O*-mesyl-β-CD (**14**, 95% yield) as the intermediate. The targeted final product **4** was obtained in a moderate yield (40%).

The preparation of per-2-*O*-alkylated compounds **5–8** required a differentiation between primary (OH-6's) and secondary hydroxyl groups (OH-2's and OH-3's) and additionally between the two types of secondary hydroxyl groups. The synthesis (Scheme 3) began with the known per-2,6-di-*O*-*tert*-butyldimethylsilylated β-CD **15**.[9a]

Under Williamson etherification conditions, the methyl groups were regioselectively introduced to the O-2 positions in 60% yield. Consistent with a previous report,[16] the 2-*O*-*tert*-butyldimethylsilyl (TBS) groups underwent a migration to the O-3 positions after treating **15** with sodium hydride. Compound **16** was obtained in 60% yield. A subsequent deprotection of the TBS groups using tetra-*n*-butylammonium fluoride (TBAF) afforded the 3,6-polyol **17** in an excellent yield (87%). Iodine-triphenylphosphine-mediated iodination[9c] successfully replaced all OH-6's with iodide leaving groups in a regioselective manner; the desired 6-heptaiodide **18** was obtained in 50% yield. Finally, the iodides in compound **18** were displaced with 1-octadecanethiolate to afford the targeted amphiphilic compound **5** in 64% yield, using conditions described above.

Attempts to prepare per-2-*O*-benzylated compound **8** from **15** by following a similar reaction sequence as shown in Scheme 3 failed to provide the per-2-*O*-benzylated intermediate in a reasonable yield. In addition, it was found to be difficult to isolate the desired compound in the pure form, as the *O*-benzylation gave a complex mixture with a close polarity which prevented an efficient separation of the desired product from other over- or under-substituted by-products. To overcome this obstacle, another route was explored using the less sterically hindered compound **19**[9a,15] that contains only seven 6-*O*-TBS groups as a starting material (Scheme 4). In fact, this compound allowed the synthesis of all remaining per-2-*O*-alkylated targets **6–8**.

Compound **19** was prepared using modified conditions.[17] Thus, the polyol (**19**) was treated with NaH (1.5 equiv. per OH-2 for **20**, 1.0 equiv. per OH-2 for **21** and **22**) in anhydrous DMF, either ethyl iodide (2.0 equiv. per OH-2) or allyl bromide (1.0 equiv. per OH-2) or benzyl bromide (1.0 equiv. per OH-2) was added and the respective mixture was stirred at room temperature overnight; the pure per-2-*O*-ethylated β-CD (**20**) was obtained in only 30% yield, while the per-2-*O*-allylated and per-2-*O*-benzylated β-CD derivatives **21** and **22** were obtained in better yields (43% for **21** and 52% for **22**). The unexpected low yield for the ethylated compound **20** was probably a result of excessive β-elimination of the electrophile (to produce ethene) during alkylation, which consumed the reagent. However, in each case, the purification of the reaction mixture was much easier, as there exists larger differences in R_fs between the desired product (**20**, **21** or **22**) and their respective over- or under-alkylated by-products in each reaction, because of the differences in the number of free hydroxyl groups; this greatly facilitated the final separation. To introduce a leaving group at the C-6 positions, all compounds **20–22** were directly converted to per-6-brominated derivatives **23–25** using an elegant

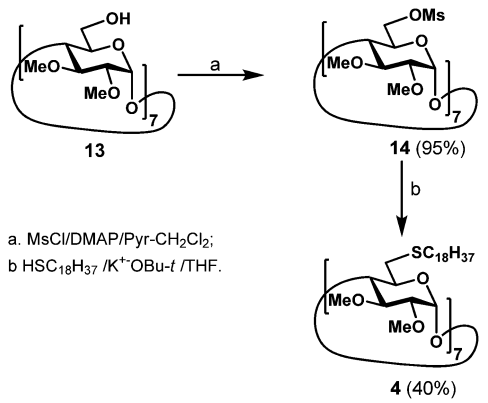

Scheme 2 Synthesis of per-2,3-di-*O*-methylated β-CD **4** from **13**.

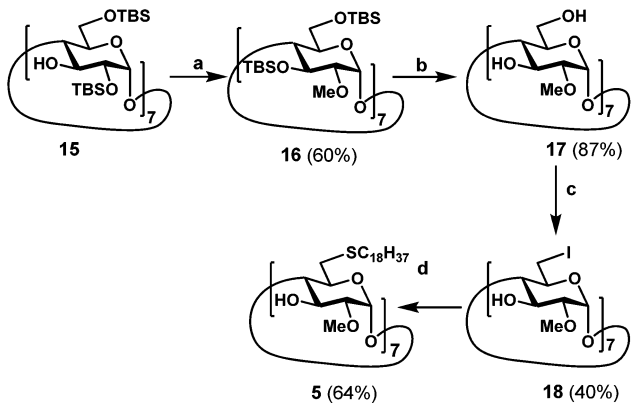

Scheme 3 Synthesis of per-2-*O*-methylated β-CD derivative **5** from **15**.

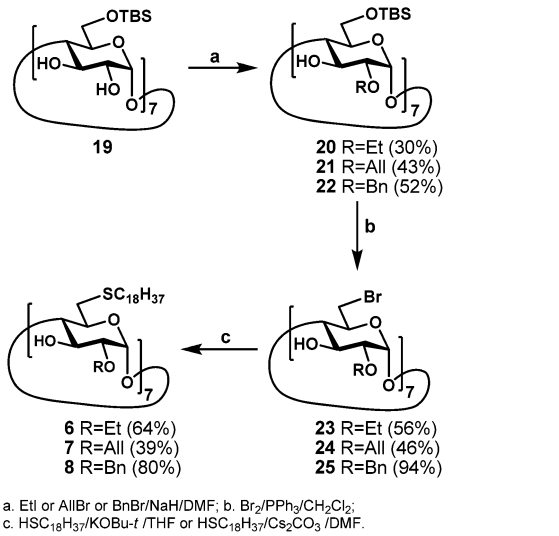

Scheme 4 Synthesis of per-2-*O*-ethylated, allylated and benzylated β-CD derivatives **6**, **7** and **8** from **19**.

approach previously reported by Darcy *et al.*[18] Thus the *tert*-butyldimethylsilyloxy groups were directly converted to 6-bromides by employing Br_2/PPh_3 as a reagent; the desired per-2-*O*-allylated (**24**) and per-2-*O*-benzylated (**25**) derivatives were isolated as precipitates by sonicating each crude reaction mixture in ethanol (46% for **24** and 33% for **25**). The per-2-*O*-benzylated compound **25** was also isolated in an excellent yield (94%) by column chromatography on silica gel using a gradient of ethyl acetate–toluene as the eluent. However, for the per-2-*O*-ethylated analog **23**, although TLC revealed that bromination worked well, it was found to be difficult to isolate the desired product in the pure form by chromatography even by using different eluents, as compound **23** had a similar polarity (R_f) to triphenylphosphine oxide which was formed as a by-product from the reaction; however, it could be precipitated out from EtOH in the pure form as above (56% yield). All per-6-bromides **23–25** very smoothly converted to the final targets **6**, **7** and **8** in moderate to good yields (64% for **6**, 39% for **7** and 80% for **8**) by reacting with 1-octadecanethiol under argon using either potassium *tert*-butoxide or cesium carbonate as a base.

The structures and purity of all target compounds **3–8** were confirmed by high resolution mass spectrometry as well as different 1D and 2D NMR experiments. For example, for the per-2-*O*-methylated, ethylated, allylated and benzylated compounds **5–8**, high resolution MALDI mass spectrometry showed the expected *m*/*z* peak of the sodium adduct in each case (see Experimental section). All 1D ^1H and ^{13}C NMR spectra of compounds **3–8** revealed the expected C_7 axial symmetry, as only one set of H-1 and C-13 signals was observed in each case, which confirmed a symmetrical substitution (see ESI†).

Mesomorphic properties

Differential Scanning Calorimetry (DSC) was performed on compounds **3–8** to determine possible thermotropic phase transitions and the associated enthalpy changes. The first heating cycle for all compounds was omitted because of thermal history. The temperatures and enthalpies of transitions from the first cooling and second heating of compounds **3–8** are summarized in Table 1. Subsequent heating and cooling cycles showed reproducible values for the phase transitions.

Dibenzylated CD **3** displayed one endothermic transition at 48.5°C on heating and an exothermic transition at 38.2 °C on cooling. Under the cross-polarized optical microscope (POM) on heating, a clear transition from the solid to isotropic liquid phase was observed. The 2,3-di-*O*-methylated β-CD analog **4** exhibited similar behaviour and displayed one endothermic transition at 53.4 °C on heating and another exothermic transition at 47.5 °C and a much smaller, broad transition at 36.5 °C on cooling; like compound **3**, the larger transitions at 47.5/53.4 °C must correspond to a phase transition between a solid and an isotropic liquid, while the smaller one should correspond to a crystal (or soft crystal) to another crystal phase. More important to note is that neither compound **3** nor **4** exhibited liquid crystallinity; this could be attributed to the absence of hydroxyl groups at the secondary face in both compounds, which eliminated their ability to self-assemble into ordered structures *via* intermolecular hydrogen bonds. In the case of compound **3**, the presence of numerous benzyl groups at the secondary face could have resulted in π–π interactions if the molecules self-assembled into a smectic LC phase. However, the results clearly indicated that such interactions were not strong enough to drive the rod-like molecules to self-organize into ordered structures.

Table 1 Phase transition temperature (°C) and Δ*H* in parentheses[a] (J g^{-1})

Compound	Heating	Cooling
3	Crys 48.5 (15.9) Iso	Iso 38.2 (15.0) Crys
4	Crys 53.4 (57.2) Iso	Iso 47.5 (51.4) Crys
5	Crys 50 (2.8) X 60 X 64.5 X 68 (31.1[b]) Sm 110 (20.7) Iso	Iso 95 (19.4) Sm 56 (36.0) X 40.5 X 37.5 (4.9[c]) Crys
6[d]	Crys 54 Sm[e] 61 Iso	Iso 51.5 Sm[e] 49 X 43.5 Crys
7	Crys 57.6 (104.9) Iso	Iso 49.7 (66.8) Crys
8	Crys 54.0 (73.3) Iso	Iso 46.7 (75.0) Crys

[a] Crys: crystalline; Iso: isotropic liquid; Sm: smectic and X: unidentified soft-crystalline phase. [b] Combined enthalpic changes of all transitions at 60, 64.5 and 68 °C. [c] Combined enthalpic changes of both transitions at 40.5 and 37.5 °C. [d] No enthalpic data are reported for compound **6** due to severe overlap of peaks in DSC thermogram. [e] Based on the structural similarity and also the formed patterns similarity (under POM) with compound **5**, the mesophase was assigned to be smectic.

Next, the thermotropic properties of compounds **5–8** were investigated. The DSC of per-2-*O*-allylated compound **7** revealed one endothermic transition at 57.6 °C on heating, and an exothermic transition at 49.7 °C on cooling; similar results were also observed for the per-2-*O*-benzylated analog **8**, which showed similar phase transitions at 54.0 °C (heating) and 46.7 °C (cooling). Under POM it was confirmed that neither compound formed LC phases, and the transitions were the results of clearing from a solid to an isotropic liquid.

The analogous compounds **5** and **6**, which had smaller groups at the O-2 position of glucopyranosyl units, exhibited distinct thermotropic behaviour. Thermogravimetric analysis revealed the per-2-*O*-methylated derivative **5** to be stable up to 250 °C (~95%) while the per-2-*O*-ethylated analog **6** to be slightly less stable – up to 200 °C (~95%). Remarkably, the DSC thermogram of compound **5** (Fig. 3) displayed five endothermic phase transitions at 50, 60, 64.5, 68 and 110 °C on the heating cycles, and four exothermic transitions at 37.5, 40.5, 56 and 95 °C on the cooling cycles; under POM it was evident that on heating the phase transition at 110 °C was the transition to the isotropic liquid. The sample was then cooled slowly at 2 °C min^{-1} from the isotropic liquid, and birefringent patterns appeared around 95 °C with characteristic fan-shaped patterns which are often seen in Sm A packing (Fig. 3). The formed mesophase appeared to be highly viscous and could be sheared. The fan-shaped patterns did not change on continuous cooling, but colours appeared gradually and after passing the transition at 56 °C, the colours became significantly brighter and rich. There was no change detected in textures under POM for the transition at 40.5 °C and 37.5 °C on cooling.

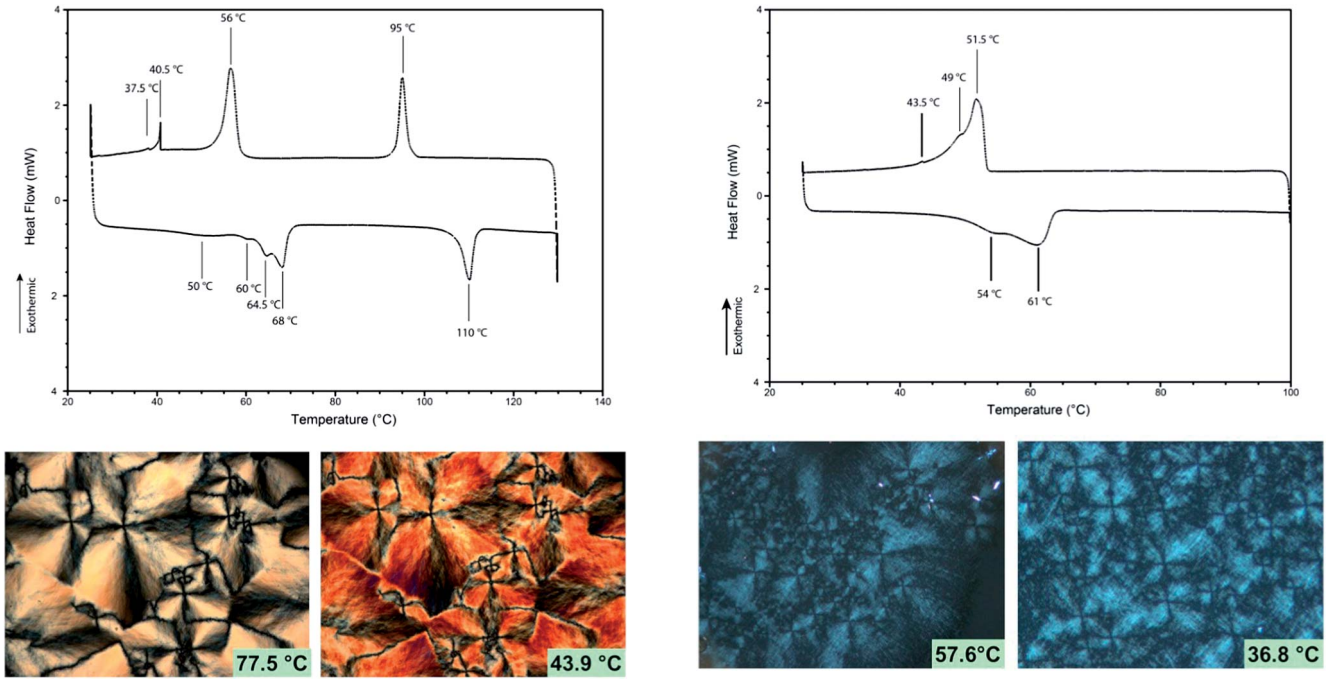

Fig. 3 DSC thermogram of compound **5** (top) after heating compound **5** to clearing temperature and allowing it to cool to room temperature at 2 °C min^{-1} and snapshots taken at 77.5 and 43.9 °C under POM.

Fig. 4 DSC thermogram of compound **6** (top) after heating compound **6** to clearing temperature and allowing it to cool to room temperature at 2 °C min^{-1} and snapshots taken at 57.6 and 36.8 °C under POM.

On the other hand, for the per-2-*O*-ethylated analog **6**, DSC detected two very broad endothermic transitions at 54 and 61 °C in the heating cycle, and three closely spaced exothermic transitions peaked at 43.5, 49 (broad), 51.5 °C (broad) in the cooling cycle. Under POM it was clear that the transition related to the peak at 61 °C on heating is the clearing temperature, and compound **6** also had liquid crystalline properties, which was evident upon cooling from ~61 °C when the similar fan-shaped birefringent patterns appeared. However, the patterns and textures remained more or less the same on further cooling (Fig. 4). Considering the structural similarity with compound **5**, the formed mesophase was assigned to be Sm packing.

DSC also provided the enthalpy change at each phase transition for compound **5**. The transitions at 56 °C in the cooling cycle had an enthalpy of 36 J g^{-1}. This value is larger than the enthalpic change (19.4 J g^{-1}) found at 95 °C (isotropic liquid to LC phase), but smaller than those observed for the melting transitions of most non-liquid crystalline compounds (**4**, **7** and **8**, 51.4–104.9 J g^{-1}). Because the liquid crystalline phase is structurally more similar to the isotropic liquid than to the crystalline phase, there is larger enthalpic change at a phase transition from LC to crystal than isotropic liquid to LC. After the transitions at 56 °C, compound **5** had crystallized at 37.5 °C. The intermediate phase transition could be between different soft crystalline phases; however, POM or XRD experiments could not conclusively identify them. For compound **6**, unfortunately, all phase transitions were broad thus unresolved; we did not attempt to integrate each transition peak to obtain the enthalpy change for individual transition.

The sharp contrast in thermotropic behaviour between compounds **5** and **6** compared to the analogous compounds **7** and **8** constitutes an interesting phenomenon. Since each of them contains seven hydroxyl groups, they should be capable of forming the same number of hydrogen bonds. However, as stated before, the difference resides in the nature of the alkyl groups attached to the O-2 positions, which vary in size. The fact that molecules substituted with smaller methyl (**5**) or ethyl (**6**) groups successfully self-organized into ordered smectic mesophases while the other two with larger substituents (allyl and benzyl, **7** and **8**) failed to do so suggests a difference in strength of intermolecular hydrogen bonds that these molecules are able to form. The derivative **5** containing the smallest substituent (methyl) showed the widest mesophase temperature range, which correlates well to its ability to allow the strongest intermolecular hydrogen bonding network to form as the small methyl group creates minimal spacing between hydroxyl groups of the adjacent layers in the smectic packing. The allyl and benzyl groups present in the other two compounds **7** and **8** respectively are probably just too large to permit the adjacent layers to get close enough to allow an effective intermolecular hydrogen-bond network to establish; thus no ordered mesophases were observed to form for either compound. Compound **6** bears seven ethyl groups whose size is intermediate from methyl to allyl; consequently, compound **6** should possess an intermediate ability to interact *via* intermolecular hydrogen-bond between adjacent layers. The reduced hydrogen-bond network is not strong enough to stabilize the mesophase at high temperatures thus much narrower temperature range was observed for the mesophase formed by compound **6** (Fig. 4).

For comparison, the previously known compound **2** that had no substituents at the secondary face was also synthesized and examined by DSC and POM. Interestingly, the DSC did not show evidence of the phase transition at 215 °C that was reported by the original publication; the DSC displayed peaks at 57 and 61 °C on heating and two corresponding peaks at 48 and 52 °C on cooling; in addition, examination of **2** under POM also did not reveal significant change in birefringence patterns around 215 °C. Based on these observations, it was suggested that the mesophase range of **2** could be even wider (57–280 °C on heating) than previously reported. This was also in agreement with the behaviour of both compounds **5** and **6**. The melting temperatures (T_m) of **2**, **5** and **6** are similar (57, 54 and ~49 °C respectively), but the clearing temperatures (T_c) are significantly altered (280 *vs.* 113 *vs.* 61 °C) by the modification on the secondary face. Since the aliphatic chain length is the same for both CD derivatives, it can be assumed that the contribution of van der Waals interactions in the smectic mesophases was similar for all three compounds. Therefore, the hydrogen bonding network that each compound is capable of establishing must account for the difference in observed T_c temperatures. More specifically, both compounds **5** and **6** have half the number of secondary OH groups as compound **2**, which should correspond to much weaker abilities of the two compounds to form a hydrogen bonding network than **2**; this was in agreement with the much lower T_c temperatures observed for compounds **5** and **6** compared to **2**.

Powder X-ray diffraction

Compound **5** was selected for analysis by powder X-ray diffraction. The phase observed between 95 and 52 °C on cooling was confirmed by (XRD) to be a smectic phase with a layer spacing of 40.7 Å; this was evidenced by the consistent presence of (001), (002), and (003) diffraction peaks whose relative intensity decreased as expected. This distance correlates well with that of analogous compound **1**, which was previously determined to have a bilayer thickness of 38 Å.[10] The addition of the methyl group plus the two extra carbons on the chains (C16 for **1** *vs.* C18 for **5**) must account for the difference. The interlayer spacing is considerably smaller than 62.2 Å (2 × 31.1 Å, Fig. 5), the length calculated for a head-to-head dimer of **5**, which likely reflects substantial interdigitation of the side chains made possible by the void associated with the CD's central cavity.

The XRD of this phase also exhibited several low intensity peaks at wider angles that could not be indexed to an LC phase. These peaks suggest some degree of three dimensional ordering within the phase, and could arise due to periodicity within the layer. As such, there is some ambiguity in the assignment of this phase as a liquid crystal; although it clearly possesses lamellar ordering, the additional peaks are suggestive of a smectic soft crystal. This assignment would also explain the relatively large enthalpy of the mesophase-to-isotropic transition, which indicates that the mesophase is highly ordered.

The XRD experiments on **5** showed that at lower temperatures (~52 °C), the compound appeared to form a long-range ordered phase; however, indexing the peaks was difficult, thus we were unable to identify this phase. The smectic ordering of the higher temperature phase was clearly disrupted, as evidenced by the disappearance of the higher order (002) and (003) peaks. The appearance of several low intensity peaks at wider angles indicates some sort of short range 3D correlation.

Packing in the LC phase

Previously, Avakyan *et al.* carried out *ab intio* and semiempirical quantum-chemical calculations[19] to look at the role of intra- and inter-molecular hydrogen bond networks in unmodified β-CD head to head dimers. As shown in Fig. 6, the secondary hydroxyl groups of two opposing CDs can establish two kinds of fairly complex hydrogen bonding networks; both involve inter- and intramolecular hydrogen bonding. For example, the OH-2 groups of one CD can simultaneously act as hydrogen bond donors by interacting with O-3's of another CD (red dotted

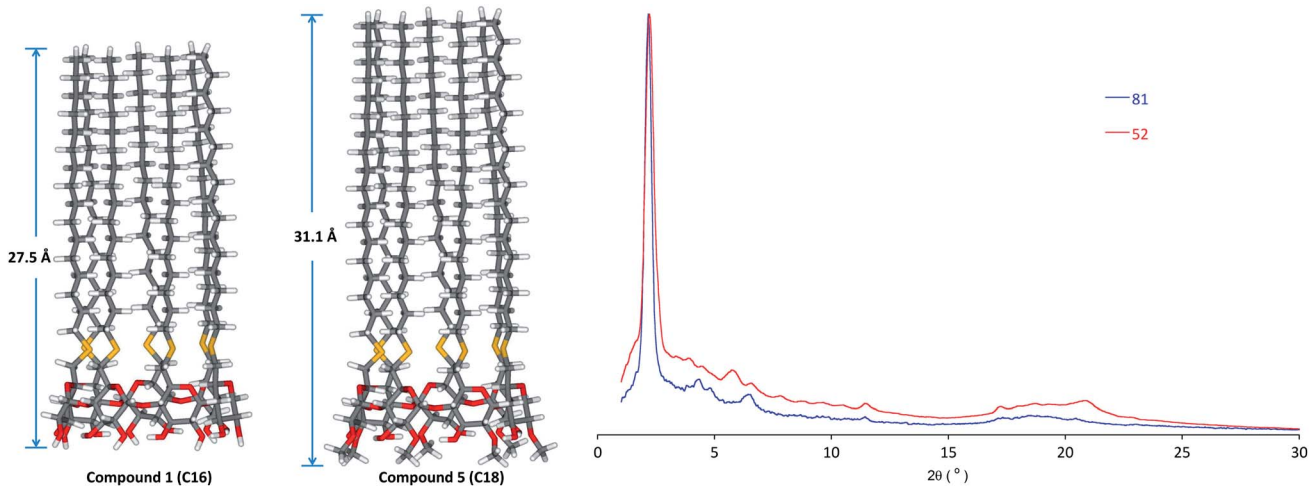

Fig. 5 Left: molecular models show compounds **1** (C16) and **5** (C18) have respectively dimensions of 27.5 and 31.1 Å in the most extended conformation. Right: variable temperature XRD plots of compound **5**, recorded at 81 and 52 °C.

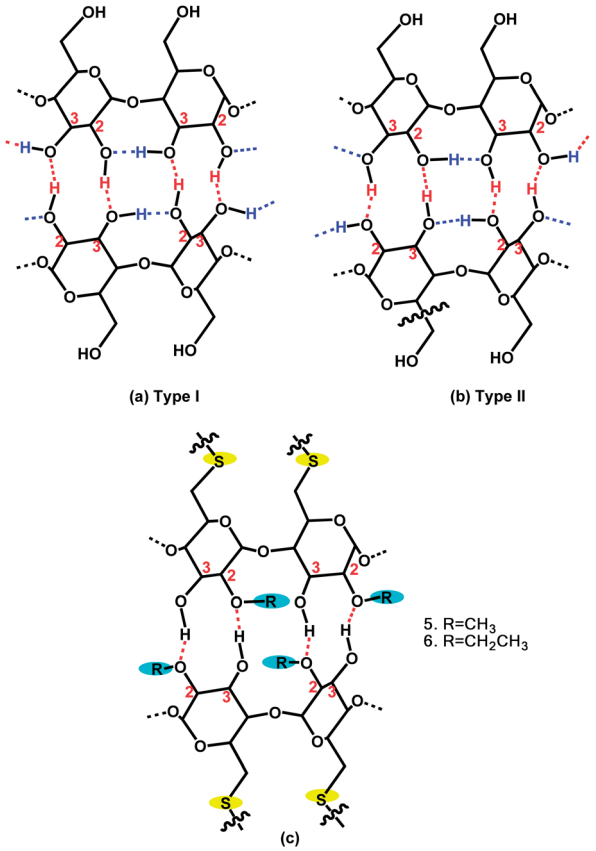

Fig. 6 Possible hydrogen-bond networks established in natural CD dimers: (a) OH-2's as intermolecular hydrogen-bond donors while OH-3's act as intramolecular hydrogen bond acceptors, (b) OH-3's act as the intermolecular hydrogen-bond donors while OH-2's act as the intramolecular hydrogen-bond acceptors, and (c) proposed hydrogen-bond network established in the dimer formed from compounds **5** and **6**.

lines), and as hydrogen bond acceptors by accepting hydrogen bonds (blue dotted lines) from an OH-3' of adjacent glucosyl units of the same CD (type I, Fig. 6a). The OH-2 and OH-3 groups can also switch roles to establish a second type of hydrogen bond network (type **II**) shown in Fig. 6b.

Avakyan *et al.*'s computational studies concluded that the type **I** hydrogen bonding network was thermodynamically more stable than the type **II**. They reasoned that the increased stability of the network in type **I** (Fig. 6a) was due to the fact that the OH-2 groups are torsionally more favoured to form stable inter-CD hydrogen bonds; in addition, the more acidic nature of the OH-2 groups compared to the OH-3's also makes them better hydrogen bond donors, leading to stronger intermolecular interactions. It can be logically assumed that the hydrogen bonding networks formed in the thermotropic LC phase of both compounds **1** and **2** resemble the network shown in Fig. 6a. However, for compounds **5** and **6**, the hydrogens in all OH-2 groups have been substituted with alkyl groups; this not only reduces the numbers of hydrogen bonds that both compounds **5** and **6** can form, but also completely removes their ability to form the more stable type **I** network. Consequently, the OH-3 groups now must dynamically act as hydrogen bond donors to interact with O-2's, both intermolecularly and intramolecularly in the bilayers, *via* the less thermodynamically stable type **II** network as shown in Fig. 6c. This model suggests a significantly reduced strength of the hydrogen-bonding network that both compounds **5** and **6** could establish, which is consistent with its observed much lower clearing temperatures, compared to compounds **1** and **2**.

We also attempted to record the FT-IR spectra of compounds **5**, **7** and **8** in order to study their differences in ability to form hydrogen-bond networks; however, due to the fact that all three compounds are able to form a strong intramolecular hydrogen bond network which interferes with the studies, our investigation did not provide conclusive results.

Conclusion

Through these studies, the role of hydrogen bonding in the self-organization of amphiphilic CDs into ordered thermotropic mesophases was clarified. It was established that modifying the secondary face to interfere with the hydrogen bonding network significantly affected the T_c of a CD amphiphiles while the T_m temperature was not greatly affected. Six new CD derivatives were designed and synthesized, and their ability to form self-organized thermotropic mesophases correlates well with their ability to form intermolecular hydrogen bonds. It was found that the synthesized CD amphiphiles need to establish a hydrogen bond network of sufficient strength to be able to drive molecules to self-assemble. A molecular model was proposed to help understand the probable packing in the mesophases for the per-6-alkylthio β-CD derivatives, and such a model also permits suggestion of a hydrogen bonding network that explains well the nature and strength of the formed hydrogen bond network. The results obtained from this study should help to design future CD-based LC materials as well as understand their thermotropic properties.

Experimental section

General methods

Analytical TLC was performed on Silica Gel 60-F_{254} (Merck, Darmstadt) with detection by quenching of fluorescence and/or by charring with 5% sulfuric acid in water or with a ceric ammonium molybdate dip. All commercial reagents were used as supplied unless otherwise stated. Column chromatography was performed on silica gel 60 (Silicycle, Ontario). Organic solutions from extractions were concentrated under vacuum at <40 °C (bath). ^{1}H NMR spectra were recorded at 400 MHz on Bruker spectrometers. The first order proton chemical shifts δ_H and δ_C are reported in δ (ppm) and referenced to either residual $CHCl_3$ (δ_H 7.24, δ_C 77.0, $CDCl_3$), residual CD_2HOD (δ_H 3.30, δ_C 49.5, CD_3OD), residual CD_3SOCD_2H (δ_H 2.50, δ_C 39.51, CD_3SOCD_3) or residual C_5D_4HN (δ_H 7.22, δ_C 123.87, C_5D_5N). ^{1}H and ^{13}C NMR spectra were assigned with the assistance of GCOSY, GHSQC spectra. Matrix-assisted laser desorption/ionization and time-of-flight mass spectra (MALDI-TOF MS) were recorded on a Bruker Daltonics AUTOFLEX III spectrometer using DHP as a matrix. High resolution ESI-QTOF mass spectra

were recorded on an Agilent 6520 Accurate Mass Quadrupole time-of-flight LC/MS spectrometer. Polarized optical microscopy was performed on OLYMPUS BX-41 equipped with a Linkam hot stage. Thermal analyses were performed using a TA-Q200 differential scanning calorimetry instrument with a heating and cooling rate of 2 °C. All data were obtained by the analytical services of the Department of Chemistry, University of Calgary.

Per-6-deoxy-2-*O*-methyl-6-octadecylthio-β-cyclodextrin (5)

A solution of compound **18** (0.178 g, 0.090 mmol) in a mixture of THF (3 mL) and CH_2Cl_2 (1 mL) was added to a solution of KOBu-*t* (0.140 g, 1.25 mmol) and thiooctadecane (0.357 g, 1.25 mmol) in THF (3 mL) under argon and the reaction mixture was heated at 65 °C for 21 h. After removing the solvents under reduced pressure, the residue was dissolved in CH_2Cl_2 (20 mL); the organic solution was washed with water (1 × 30 mL) and dried over anhydrous magnesium sulfate and evaporated. The residue was purified by column chromatography on silica gel using 1% MeOH–CH_2Cl_2 as an eluent to afford compound **5** as a white solid (0.175 g, 64.4% yield). R_f 0.45 (MeOH–CH_2Cl_2, 5 : 95). $[\alpha]_D$ +58.6 (*c* 0.9, $CHCl_3$). ^{1}H NMR ($CDCl_3$, 400 MHz) δ 5.02 (d, J = 3.4 Hz, 7H, 7 × H-1), 3.92 (dd, J = 9.3, 9.3 Hz, 7H, 7 × H-3), 3.89–3.82 (m, 7H, 7 × H-5), 3.66 (s, 21H, 7 × OCH_3), 3.50 (dd, J = 9.1, 9.1 Hz, 7H, 7 × H-4), 3.27 (dd, J = 9.7, 3.5 Hz, 7H, 7 × H-2), 3.04–2.88 (m, 14H, 7 × H-6a + 7 × H-6b), 2.60 (t, J = 7.4, 14H, 7 × S–CH_2), 1.63–1.51 (m, 14H, 7 × S–CH_2CH_2), 1.43–1.33 (m, 14H, 7 × S–CH_2CH_2CH_2), 1.35–1.20 (m, 196H, alkyl), 0.89 (t, J = 6.7 Hz, 21H, 7 × CH_3). ^{13}C NMR (CD_3OD, 100 MHz) δ 100.91 (C-1), 85.80 (C-4), 82.12 (C-2), 72.98 (C-3), 70.96 (C-5), 60.35 (OCH_3), 33.79 (C-6), 33.71 (S–CH_2), 31.94, 29.93, 29.82, 29.76, 29.69, 29.49, 29.38, 29.10, 22.69, 14.11. *m*/*z* (HRMS MALDI-TOF) calcd for $[C_{1175}H_{336}O_{28}S_7 + Na]^+$ 3133.2805, found: 3133.2754.

Per-6-deoxy-2-*O*-ethyl-6-octadecylthio-β-cyclodextrin (6)

Compound **23** (50 mg, 28 μmol) was dissolved in a mixture of anhydrous DMF (1.5 mL) and THF (1 mL) under argon; 1-octadecanethiol (113 mg, 0.40 mmol) and Cs_2CO_3 (125 mg, 0.40 mmol) were added and the reaction was heated to 60 °C for 2 days. Then the temperature was raised to 80 °C for 1 h. The reaction mixture was diluted with EtOAc (20 mL) and washed with H_2O (1 × 40 mL), saturated brine (2 × 40 mL) and dried over anhydrous Na_2SO_4. After concentration under reduced pressure, the crude mixture was purified by column chromatography on silica gel using EtOAc–toluene (15 : 85) as the eluent to afford pure compound **6** as a white solid (58 mg, 64% yield). R_f 0.24 (EtOAc–toluene, 20 : 80). ^{1}H NMR (400 MHz, $CDCl_3$) δ 5.08 (s, 7H, 7 × OH-3), 4.97 (d, J = 3.5 Hz, 7H, 7 × H-1), 4.06 (dq, J = 7.1, 9.3 Hz, 7H, 7 × OC*Ha*HbCH$_3$), 3.97–3.80 (m, 14H, 7 × H-3 + 7 × H-5), 3.72 (dq, J = 7.1, 9.3 Hz, 7 × OCHa*Hb*CH$_3$), 3.47 (dd, J = 9.2, 9.2 Hz, 7H, 7 × H-4), 3.35 (dd, J = 9.6, 3.4 Hz, 7H, 7 × H-2), 3.00 (dd, J = 2.2, 13.8 Hz, 7 × H-6a), 2.93 (dd, J = 5.3, 13.8 Hz, 7 × H-6b), 2.60 (t, J = 7.4 Hz, 14H, S–CH_2), 1.63–1.53 (m, 14H, 7 × S–CH_2CH_2), 1.47–1.16 (m, 231H, 7 × S–CH_2CH_2(CH_2)$_{15}$ + 7 × OCHaHbCH_3), 0.89 (t, J = 6.7 Hz, 21H, 7 × CH_3). ^{13}C NMR (100 MHz, $CDCl_3$) δ 101.56 (C-1), 85.83 (C-4), 80.24 (C-2), 73.09 (C-3), 70.81 (C-5), 68.25 (OCHaHb), 33.86 (C-6), 33.66 (S–CH_2), 31.92, 29.91, 29.81, 29.80, 29.78, 29.75, 29.67, 29.48, 29.37, 29.09, 22.67, 15.26 (OCHaHb*C*H$_3$), 14.09 (CH_3). *m*/*z* (HRMS MALDI-TOF) calcd for $[C_{182}H_{350}O_{28}S_7 + Na]^+$ 3231.3906, found: 3231.4020.

Powdered X-ray crystallography

Samples were heated to the isotropic liquid phase on a hot plate and loaded by capillary action. The excess material was cleaned off the sides with clean dry tweezers. Capillaries were then cut to length and mounted in a capillary furnace.[20] Measurements were carried out on a Rigaku RAXIS rapid diffractometer using Cu Kα radiation (λ = 1.5418 Å), a graphite monochromator and a Fujifilm Co. Ltd curved image plate (460 mm × 256 mm). Temperature was controlled with an Omega temperature controller connected to the capillary furnace with a K-type thermocouple for feedback. Owing to technical issues, the controller was set to manual mode. Due to thermal equilibration, the temperature often dropped during the course of acquisition. Only the final temperature is reported. A 0.3 mm collimator was used and all samples were irradiated for 30 minutes. Peaks and their respective angle measurements and *d*-spacings were determined using the MDL JADE software. The peak type was analysed by taking the reciprocal *d*-spacings and dividing them by the highest intensity peak, unless otherwise noted. Only peaks with greater than 1% intensity in the low angle region were analysed.

Acknowledgements

We thank both referees for the insightful reviews and suggestions and we acknowledge stimulating discussions with Drs Todd Sutherland and Robert Lemieux. We are grateful to Dr Thomas Baumgartner for the use of the TA-Q200 differential scanning calorimetry instrument. The financial support from Alberta Innovates – Technology Futures, the Natural Sciences and Engineering Research Council of Canada, and the University of Calgary are greatly acknowledged.

Notes and references

1 (*a*) C. Tschierske, *Prog. Polym. Sci.*, 1996, **21**, 775–852; (*b*) J.-M. Lehn, *Angew. Chem., Int. Ed.*, 1990, **29**, 1304–1319; (*c*) P. Metrangolo, F. Meyer, T. Pilati, G. Resnati and G. Terraneo, *Angew. Chem., Int. Ed.*, 2008, **47**, 6114–6127; (*d*) H. Ringsdorf, B. Schlarb and J. Venzmer, *Angew. Chem., Int. Ed.*, 1988, **27**, 113–158.

2 T. Kato, N. Mizoshita and K. Kishimoto, *Angew. Chem., Int. Ed.*, 2006, **45**, 38–68.

3 S. Sergey, P. Wojciech and G. Y. Henri, *Chem. Soc. Rev.*, 2007, **36**, 1902–1929.

4 (*a*) C. M. Paleos and D. Tsiourvas, *Liq. Cryst.*, 2001, **28**, 1127–1161; (*b*) T. Kato, N. Mizoshita and K. Kanie, *Macromol. Rapid Commun.*, 2001, **22**, 797–814; (*c*) T. Kato, *Struct. Bonding*, 2000, **96**, 95–146.

5 G. A. Jeffrey, *Acc. Chem. Res.*, 1986, **19**, 168–173.

6 J. W. Goodby, V. Goertz, S. J. Cowling, G. Mackenzie, P. Martin, D. Plusquellec, T. Benvegnu, P. Boullanger, D. Lafont, Y. Queneau, S. Chambert and J. Fitremann, *Chem. Soc. Rev.*, 2007, **36**, 1971–2032.
7 H. A. van Doren, E. Smits, J. M. Pestman, J. B. F. N. Engberts and R. M. Kellog, *Chem. Soc. Rev.*, 2000, **29**, 183–199.
8 F. Sallas and R. Darcy, *Eur. J. Org. Chem.*, 2008, 957–969.
9 For examples of perfunctionalization methods of cyclodextrins, see: (*a*) P. Fugedi, *Carbohydr. Res.*, 1989, **192**, 366–369; (*b*) A. W. Coleman, P. Zhang, C.-C. Ling and H. Parrot-Lopez, *Carbohydr. Res.*, 1992, **224**, 307–309; (*c*) A. Gadelle and J. Defaye, *Angew. Chem., Int. Ed.*, 1991, **30**, 78–80; (*d*) D. A. Fulton and J. F. Stoddart, *J. Org. Chem.*, 2001, **66**, 8309–8319; (*e*) S. Ward and C.-C. Ling, *Eur. J. Org. Chem.*, 2011, 4853–4861; (*f*) P. Zhang, A. Wang, L. Cui and C.-C. Ling, *Org. Lett.*, 2012, **14**, 1612–1615.
10 C.-C. Ling, R. Darcy and W. Risse, *Chem. Commun.*, 1993, 438–440.
11 (*a*) L. Chen, T.-H. Hu, H.-L. Xie and H.-L. Zhang, *J. Polym. Sci., Polym. Chem. Ed.*, 2010, **48**, 2838–2845; (*b*) J. Terao, S. Tsuda, Y. Tanaka, K. Okoshi, T. Fujihara, Y. Tsuji and N. Kambe, *J. Am. Chem. Soc.*, 2009, **131**, 16004–16005.
12 T. Sato, H. Nakamura, Y. Ohno and T. Endo, *Carbohydr. Res.*, 1990, **199**, 31–35.
13 P. Angibeaud and J. P. Utille, *Synthesis*, 1991, 737–738.
14 E. Zaborova, J. Deschamp, S. Guieu, Y. Bleriot, G. Poli, M. Menand, D. Madec, G. Prestat and M. Sollogoub, *Chem. Commun.*, 2011, **47**, 9206–9208.
15 K. Takeo, H. Mitoh and K. Uemura, *Carbohydr. Res.*, 1989, **187**, 203–221.
16 P. R. Ashton, S. E. Boyd, G. Gattuso, E. Y. Hartwell, R. Koniger, N. Spencer and J.-F. Stoddart, *J. Org. Chem.*, 1995, **60**, 3898–3903.
17 P. Zhang, C.-C. Ling, A. W. Coleman, H. Parrot-Lopez and H. Galons, *Tetrahedron Lett.*, 1991, **32**, 2769–2770.
18 C. Byrne, F. Sallas, D. K. Rai, J. Ogier and R. Darcy, *Org. Biomol. Chem.*, 2009, **7**, 3763–3771.
19 V. G. Avakyan, V. B. Nazarov, M. V. Alfimov, A. A. Bagatur'yants and N. I. Voronezheva, *Russ. Chem. Bull.*, 2001, **50**, 206–216.
20 C. Lavigueur, E. J. Foster and V. E. Williams, *J. Appl. Crystallogr.*, 2008, **41**, 214–216.